DETERMINATION OF CORROSION INITIATION OF REBAR IN CONCRETE BY MONITORING HALF-CELL POTENTIAL

G. M. Sadiqul Islam[1*], Takafumi Sugiyama[2]

[1] PhD Research Student, Division of Civil Engineering
School of Engineering, Physics and Mathematics
University of Dundee, Dundee DD14HN, United Kingdom

[2] Professor, Environmental Material Engineering Laboratory, Graduate School of Engineering,
Hokkaido University, Sapporo, 060-8628, Japan.

*Corresponding Author: gmsislam@yahoo.com

Abstract: Corrosion of rebars in concrete is a key mechanism which determines the durability and service life of concrete structure. Half-cell potential of rebars in concrete subjected to a NaCl solution of 10% in the concentration has been monitored using embedded reference electrode in the concrete and computer operated automatic data acquisition system. A portable corrosion meter was also employed to measure half-cell potential and AC impedance. Initiation of corrosion in rebars were estimated by the former system and verified by the later. Corrosion initiation period was found to be from as early as 119 days and up to 360 days of chloride application depending on the characteristics of test specimens. Upon successful detection of corrosion initiation threshold chloride concentration for corrosion initiation was estimated. The estimated chloride threshold level for deformed rebar was found almost half of that with ideal plain steel rebar. Corrosion was spread over rebars depending on its surface characteristics.

Keywords : *Half-Cell Potential; Embedded Reference Electrode; Portable Corrosion Meter; AC Impedance; Corrosion.*

1.0   Introduction

In a chloride-laden environment the presence of adequate moisture and oxygen causes localized break in alkali protected film and initiate corrosion of rebars in concrete when chloride concentration goes above a critical concentration (Chloride Threshold Level, CTL) (Tuutti 1982; Masi et al., 1997). To predict the long term performance of concrete structures under chloride laden environments it is necessary to clarify the threshold chloride concentration for the initiation of corrosion of rebars in the concrete. A considerable number of researches have been done in connection with chloride penetration in various concrete

compositions (Masi et al., 1997; Bertolini et al., 2004). Several researches also reported chloride threshold concentration for corrosion initiation of rebars in concrete in various environmental conditions (Xua and Wand, 2009; Manera et al., 2008). The first attempt to measure CTL was using a synthetic concrete pore solution with a $[Cl^-]:[OH^-]$ ratio of 0.6 using half cell potential as a tool for corrosion detection (Hausmann, 1967). Later other electrochemical tools were used for CTL measurement e.g. polarization (Yonesawa et al., 1988; Alonso et al., 2002), macrocell current (Hansson and Sorensen, 1990; Schiessl and Raupach, 1990), AC impedance (Hope and Ip, 1989). An extensive experimental work was carried out on different concrete in marine environment and CTL values are calculated from mass loss of rebars (Thomas, 1996). Chloride attack in the existing real concrete structures also studied (Vassie, 1984). Due to the variation in test procedure and exposure condition, all the reported CTL values varied in a wider range. Also none of the reported values are obtained from a real time corrosion monitoring system. Despite of wider range of reported values, most of the current design codes are using conservative values to ensure safety and serviceability of concrete structures throughout the whole service life.

To date the research field on corrosion of rebars in concrete lacks on reliable method for the detection of corrosion initiation of rebars in concrete. A method using embedded lead reference electrode inside concrete for detection of corrosion initiation of rebars in concrete has been proposed recently (Horiguchi et al., 2006; 2007). The lead reference electrode monitors the half-cell potential of steel reinforcement inside the concrete. Corrosion initiation is predicted from the sharp fall of half-cell potential to a considerable negative value. However it is need to verify the effectiveness of this system to use in corrosion research in terms of other electrochemical parameters (e.g. corrosion current) and extent of detection level. Furthermore, in recent years durability of reinforced concrete is proposed to consider as a performance based approach. It is demanded to consider the concrete mix proportions for CTL measurement. Earlier research with synthetic pore solution also pointed that the initiation of corrosion occurs followed by increase in chloride concentration and consequent drop in alkalinity adjacent to rebars (Mammoliti et al., 1996). Kayyali and Haque (1988) attempted to correlate Cl^- and OH^- for corrosion of rebar from pore solution analysis of cement paste.

This research principally aimed to establish a test method to point out the initiation of corrosion of rebars in concrete reliably. A combination of two different systems is proposed to detect the corrosion initiation and its rate estimation. Thereafter, chloride threshold level was determined for two different mixes proportioned Ordinary Portland Concrete (OPC). In connection with this the $Ca(OH)_2$ was quantified at the vicinity of rebars using a Thermo-

Gravimetry/Differential Thermal Analyzer (TG/DTA). Finally, the concentration of OH⁻ and Cl⁻ is correlated as a corrosion initiation criterion.

2.0   Experimental Program

2.1   *Materials and mix proportions of concrete*

Two types of Ordinary Portland Cement (OPC) concrete (N2 and N1) were used in this study. Details of mix proportions and concrete properties are given in Table 1. Ordinary Portland Cement (OPC) of density 3.16 g/cm^3 was used to prepare the specimens. The coarse aggregate was crushed stone with a maximum size of 13 mm. Chloride free sand collected from Mukawa River, Japan was used as fine aggregate. Absorption and specific gravity of coarse and fine aggregate were 1.62% & 2.85% and 2.68 g/cm^3 & 2.61 g/cm^3 respectively. Fineness moduli of coarse and fine aggregate were 6.10 and 2.68 respectively.

Table 1 : Mix proportions and properties of concrete

Type	G_{max}[1]	Target Slump	Target Air	W/C	s/a[2]	Unit weight (kg/m^3)				Chemical admixtures	
										AE1[a]	AE2[b]
	mm	mm	%	%	%	W[3]	C[4]	S[5]	G[6]	g/m^3	g/m^3
N1				65	46	161	248	879	1028	2.48	8.67
N2	13	120±15	5±0.5	50	43	162	324	793	1047	3.24	11.34

[1]Maximum coarse aggregate size, [2]Sand aggregate ratio, [3]Water, [4]Cement, [5]Sand, [6]Gravel, [a]AE1: Pozzolith 78S (Water reducer), [b]AE2: Micro air 785

2.1.   *Reinforcing bars and reference electrode*

A total of 14 specimens were prepared using plain or deformed round steel rebar. Among those, 11 specimens contained plain rebars (five of them also contained lead reference electrode) and 3 contained ordinary deformed steel bar with mill scale. Both type rebars had a nominal diameter of 19 mm. Electrical connection at the rebar end was made with self-tapping screw and sealed electrical copper wires. Both the electrical connected and non-connected ends of a bar were sealed with epoxy resin on the second day of concrete casting before starting curing.

Several types of reference electrodes were used for half-cell potential measurement in different conditions those includes Cu/CuSO$_4$ reference electrode in ASTM standard C876, saturated calomel electrode (SCE) in the study by Hussain et al. (1996) and Ag/AgCl reference electrode by Montemor et al. (2006). However, stability of reference electrode inside concrete is still under

question. In this study, specially designed Pb/PbO_2 reference electrode was placed inside five N2 concrete specimens before casting. Stability of the lead reference electrode in high alkaline environment is tested and confirmed by the manufacturer. The electrode was hold in exact position during casting by means of a plastic rod (Φ8 mm). Details of specimens with reference electrode placement can be found in Figure 1. Care has been taken during concrete placement and compaction to avoid the electrode displacement from original position and any disturbance in electrical connection.

2.2. *Specimen preparation*

Four types of specimens were prepared (e.g. N1P, N2P, N2PS and N2D). Configuration details are shown in Table 2. Each specimen contains two rebars at 20 mm (named 'UP') and 25 mm (named 'DO') cover distance from the top surface. It was expected that chloride ion will induce corrosion in UP rebar while DO will remain uncorroded in some time span. Specimens without reference electrode are having the same configuration as shown in Figure 1. The concrete was mixed with a biaxial concrete mixture.

(a)   (b)
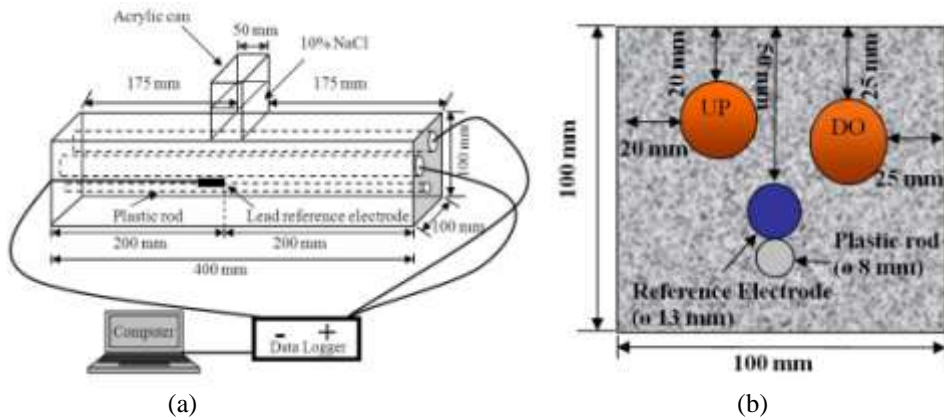
Figure 1 : (a) Details of corrosion monitoring system; (b) Cross-section of test specimen

Table 2 : Corrosion test specimen configuration

Specimen series		No of specimen	Contents	Remark
N1P		3	Plain bar	W/C = 65%
N2P		3	Plain bar	
	N2D	3	Deformed bar	W/C = 50%
N2PS		5	Plain bar & RE[1]	

[1] Reference electrode

To avoid bleeding water to accumulate underneath the rebars, concrete was placed in lengthwise direction. Internal poker vibration was used to compact the N1P, N2P and N2D specimens and formwork vibration has been used to compact the N2PS specimens. All specimens were cured in a temperature controlled water tank for 28 days. Then all sides (except top and bottom) of the specimens were sealed with water proof tape. An acrylic canister (50×100 mm in cross section) was set on the middle of each specimen (Figure 1a) with glue. Thereafter, NaCl solution of 10% in concentration was poured in that can and all specimens were placed in a temperature controlled room. N2PS specimen series were connected with the computer operated automatic data acquisition system.

NaCl solution inside the canister was maintained to approximately 50 mm in height by recharging distilled water every week during test period to avoid change in solution concentration due to evaporation of water.

2.3   Measurement

2.3.1   Electrochemical data and corrosion diagnosis

Half-cell potential and ambient temperature of N2PS specimens were obtained continuously at an interval of 8 hours. To monitor and control temperature in test room, A J type thermocouple was coupled with the data acquisition system. A portable corrosion meter was used to measure the half-cell potential and AC impedance in 1-2 month interval for all the specimens. During measurement, this device first obtains the AC impedance measurement at 13 different frequencies ranging from 10 mHz to 10 Hz, followed by the half-cell potential measurement with respect to a Ag/AgCl reference electrode. For AC impedance measurement a Double-Counter Electrode (DCE) is used. Working principal and data analysis method using DCE are referred to (Yokota, 1998; Sorn et al., 2001). To obtain impedance data and half-cell potential the double counter electrode was placed at the top surface where NaCl was applied to the specimen and noted as 'UM' and 'DM' for the 20 mm and 25 mm cover bar respectively. A sharp drop in half-cell potential was observed by the lead reference electrode/portable corrosion meter at certain age of chloride application.

2.3.2   Corrosion Area Measurement

Rebar corrosion area was measured followed by cutting and splitting of corrosion test specimens. In general, corrosion initiation was found on rebars surface beneath the 50 mm width of chloride application zone. The rebar surface

was cleaned carefully except the corrosion initiated zone. A transparent type marking tape of width 50 mm was wrapped carefully on the circumferential surface of corroded rebars. Then using a fine tip permanent black marker pen corrosion area was sketched carefully. The tape was detached from the rebar surface and associated carefully on a thick white paper. An image of this paper has been produced by scanning the paper. Computer image analysis software (Image J) has been used to quantify the corrosion area.

2.3.3   Determination of chloride ion concentration

After successful detection of corrosion onset by the lead reference electrode/portable corrosion meter or both, concrete specimens were taken from the middle of the test specimen (50 mm in width) for chloride analysis. It was cut in an approximately 5 mm layers from chloride application surface to vertically down direction using a diamond type micro cutter. Conventional acid extraction method was employed to extract chloride from approximately 10 gm of powered sample (JIS, 2003). Thereafter an automatic chloride ion titration device was used to measure the chloride ion concentration in each layer of concrete specimen. There was some time lag between the estimated corrosion initiation time and chloride profiling. Experimental data obtained from the titration were automatically fitted with the solution of Fick's 2nd law using computer software. Total of estimated corrosion initiation time and the time lag in chloride profiling was used for the non linear regression analysis. The surface chloride ion concentration and diffusion coefficient were found from the fitting. Then using obtained diffusion coefficient and surface chloride ion concentration another curve was fitted considering the estimated corrosion initiation period.

2.3.4   Quantification of Ca(OH)$_2$ using TG/DTA

In this study, quantification of the $Ca(OH)_2$ in concrete sample was done by using TG/DTA. Concrete samples were taken from the vicinity of rebar corrosion zone of test specimens. The concrete sample was grinded to powder form for analysis. Analysis was carried out at a temperature range of 20 - 1000 °C with an increment rate of 10 °C/min. Nitrogen (N_2) gas was used for the test with a flow rate of 200 ml/min. Alumina (Al_2O_3) was used as a reference weight to the concrete samples. The DTA graph indicates dehydroxylation of $Ca(OH)_2$ which formed during hydration. $Ca(OH)_2$ was estimated from the weight loss measured from the TG curve at corresponding DTA peak. Gravimetric relationship among $Ca(OH)_2$, CaO and H_2O were used in calculation. Further gravimetric calculation on $Ca(OH)_2$ gave quantity of OH^- in concrete.

3.0   Experimental results and discussion

3.1. *Properties of fresh and hardened concrete*

Slump and air content of test concrete was measured during batching. Compressive strengths were determined from the test cylinders after 28 days and 91 days water curing. All the properties of test concrete are summarized in Table 3.

Table 3 : Properties of fresh and hardened concrete

Concrete type	Slump (mm)	Air content (%)	Compressive Strength (MPa)	
			28 days	91 days
N1	105	5.5	28.1	33.4
N2	130	5.3	42.9	48.4

3.2. *Estimation of corrosion onset and its nature*

Continuous monitoring of half-cell potential of five N2PS samples is shown in Figure 2. At the beginning, the half-cell potential was found in a steady condition with time. In some certain age of chloride application it was found that the half-cell potential was dropped to a considerable negative value from the steady condition within a couple of hours. ASTM C876 (1999) criteria was used to assess the corrosion initiation state.
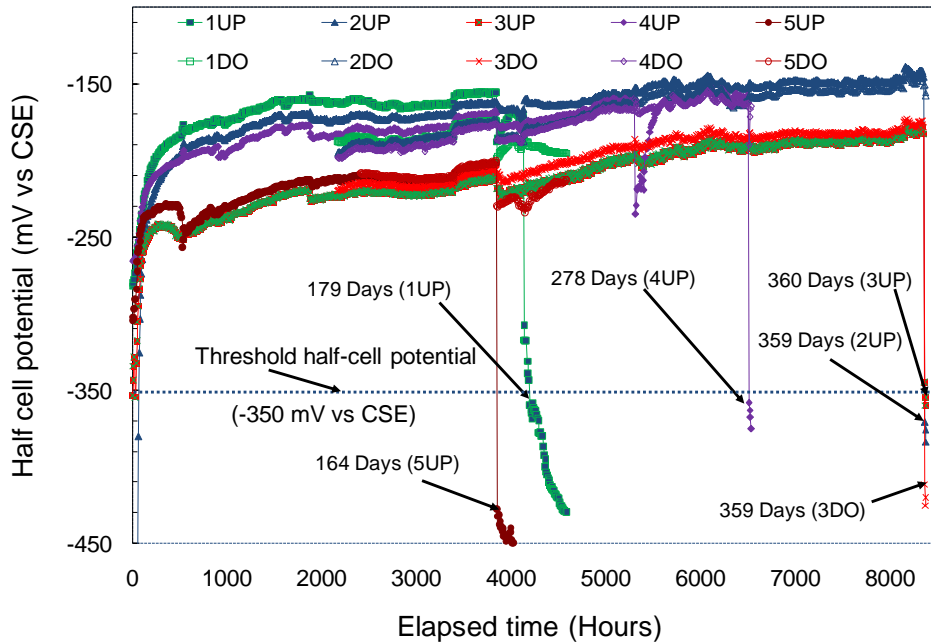
Figure 2: Half-cell potential monitoring by embedded reference electrode in N2PS samples

The threshold half-cell potential (*Ecorr* of -350 mV vs CSE, where the standard says more than 90% probability of corrosion occurrence) is shown using a dotted line. Half-cell potential of the UP bar of specimen 1 and 5 dropped below the threshold half-cell potential early at 179 days (4296 hours) and 164 days (3944 hours) respectively which indicates corrosion initiation in these bars, while no drop was observed in the DO rebar of the same specimens. Specimen 4 took an intermediate time of 278 days (6680 hours) to initiate corrosion.

Corrosion estimated in specimen 2 and 3 at a considerable longer time of 359 days (8616 hours) and 360 days (8624 hours) respectively. As the UP bar has 5 mm lower cover than the DO bar it was expected that the DO bar will remain uncorroded over a time span while the UP initiate corrosion. All the five specimens except specimen 3 supported the hypothesis precisely. Estimation of corrosion initiation is cross checked with the obtained half-cell potential by portable corrosion meter. Thereafter, the specimens were cut and split to confirm corrosion by visualization. Corrosion initiation of the specimens (N1P, N2P and N2D) was estimated from the periodic half-cell potential measurement (1-2 months interval) by the portable corrosion meter instead of continuous monitoring. The corrosion initiation period were estimated as average of the

chloride application period when half-cell potential dropped below the threshold half-cell potential and the last measurement time when no significant drop in half-cell potential was observe. Corrosion current was estimated from the obtained cole-cole plot of AC impedance spectroscope. Half-cell potential, corrosion current and corrosion initiation period are summarized in Table 4.

The corrosion monitoring system detected corrosion in specimens 1 and 5 of N2PS series at a comparatively early age. Corrosion current at UM position of specimen 1 and 5 were found 0.123 $\mu A/cm^2$ and 0.057 $\mu A/cm^2$ respectively which are considerably higher than the other samples of the same series at the stage of initiation. One possible cause could be the presence of various sized air voids which were found in the concrete and rebar interface of these two specimens as shown in Figure 3. During casting of concrete against a steel bar, a dense continuous cement rich layer containing rich precipitation of calcium hydroxide is postulate to be formed at the steel–concrete interface (Page, 1975). This layer restricts the tendency for a decrease in pH at anodic areas and also reduces the mobility of chloride ions (Page and Treadaway, 1982).

Table 4 : Half-cell potential (Ecorr), corrosion current (Icorr) and corrosion initiation period

Series	Specimen name	Estimated corrosion initiation time (Days)	E_{corr} (mV vs CSE)		I_{corr} ($\mu A/cm^2$)	
			UM position	DM position	UM position	DM position
N2PS	N2PS1	179	-488	-253	0.123	*
	N2PS2	359	-381	-164	0.022	*
	N2PS3	360	-349	-410	0.007	0.016
	N2PS4	277	-415	-249	0.002	*
	N2PS5	164	-510	-257	0.057	*
N2P	N2P1	191	-477	-218	0.036	*
	N2P2	298	-512	-239	0.938	*
	N2P3	251	-202	-465	0.068	0.096
N2D	N2D1	119	-467	-227	0.152	*
	N2D2	119	-504	-223	0.155	*
	N2D3	119	-608	-555	0.207	0.089
N1P	N1P1	119	-572	-268	0.287	*
	N1P2	119	-524	-534	0.179	0.168
	N1P3	119	-579	-589	0.382	0.241

* No corrosion initiation.

Corrosion initiates from the weakest surface, often presents in terms of air voids. Interface of those two specimens contained air voids, the specific zone was lacking from sufficient alkalinity required to resist corrosion initiation. Also accelerated corrosion rate was found at initiation due to this phenomenon. Lowest corrosion current estimated by the system among the test specimens is at UM position of N2PS4 sample was 0.002 μA/cm^2.

Due to having a sound interface (see Figure 3) corrosion initiation was with the lowest corrosion current and after a considerable period of chloride application compared to the other two specimens discussed earlier. The above discussion also supports the initiation of corrosion in specimen 2 and 3 at longer time with lower corrosion current. A sound and dense interface were found for these specimens also. Figure 3 also shows an example of clear corrosion initiation in the UM position while the DM position of rebars remains intact.

N2PS1UM   N2PS5UM   N2PS4UM   N2PS2
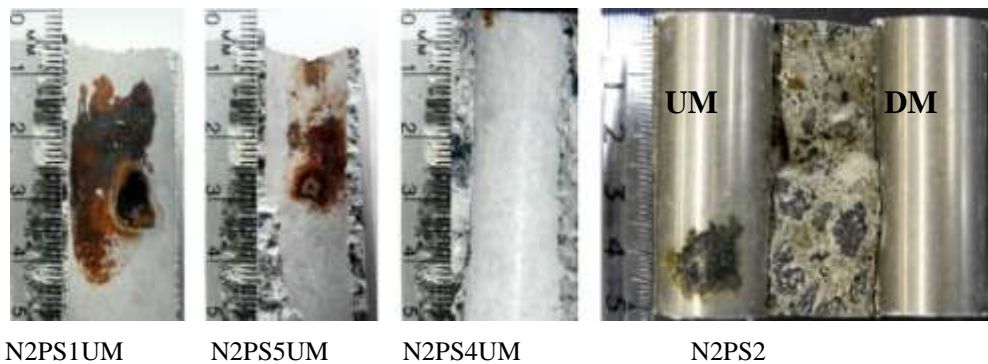
Figure 3 : Rebar and concrete interface of N2PS1, N2PS5 and N2PS4 and corrosion N2PS2

3.3. *Assessment of corrosion onset nature in terms of area of corrosion*

Rebar corrosion area for one deformed and one plain rebar are demonstrated in Figure 4. At the stage of corrosion initiation rebar corrosion area of N2PS series was ranged from 0.08 – 0.67 cm^2. Average corrosion area (0.36 cm^2) of N2PS series is the lowest among the four series of test specimen. This assesses the accuracy of detection of corrosion initiation with proposed corrosion monitoring system. Considering rebars placed at the same depth in different series of corrosion test specimens an average corrosion area was found for 7.25, 2.43, 1.90, and 0.36 cm^2 for specimen series N2D, N1P, N2P, N2PS, respectively

which gives order of corrosion area as N2D>N1P>N2P>N2PS. As shown in Table 4, the corrosion current (rate) was found highest in the N1P specimen series. However the corrosion area in N2D series found highest among all the groups. As shown in Figure 4, the ribs of deformed rebars are affected severely. Presence of extended ribs would be responsible for an uneven concrete and steel interface. Although concrete is placed in a lengthwise direction, it seems that the bleeding water accumulated underneath the ribs and caused voids in the hardened concrete.

(a)   (b)
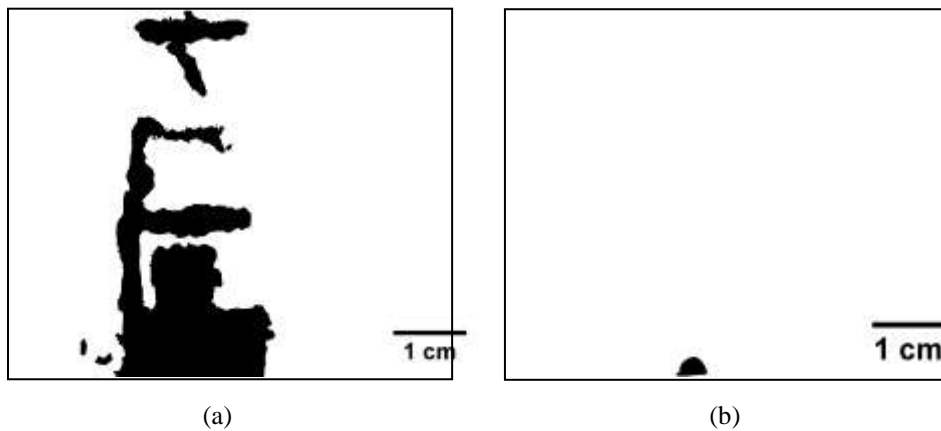
Figure 4 : Corrosion area (a) N2D3 UP and (b) N2PS4 UP

Also the presence of weaker and uneven interfacial zone probably resulted corrosion initiation in N2D specimens earlier. Studies carried out with deformed bars also postulated higher corrosion rate in deformed rebars compared to plain steel bars (Mohammed et al., 1999).

From the above discussion it is clearly understandable that corrosion initiation detected in N2PS series of specimens with lead reference electrode at lowest possible corrosion current (rate) and area of corrosion. Also the accuracy of corrosion initiation detection affects the reliability of test results as after corrosion initiation it accelerates rapidly.

3.4. *Chloride threshold level*

The obtained chloride profile gives chloride concentration at different depth at the estimated corrosion initiation time. As mentioned earlier corrosion was initiated at UP position in some of the specimens and both UM and DM position

was corroded in other specimens. The chloride threshold value was estimated as chloride concentration at 20 mm depth if UM position confirms initiation of corrosion only and at 25 mm depth if both the bars confirm corrosion. Summary of chloride analysis for different series of specimens is presented in Table 5. Although same N2 type concrete was used for N2P, N2PS and N2D series of specimens, the chloride threshold level was found almost half for N2D series compared to other two. Earlier studies also indicated that deformed bars starts corrosion with lower chloride concentration and once corrosion starts the propagation rate also higher for deformed rebars (Mohammed et al., 1999, Hansson and Sørensen, 1990; Poursaee and Hansson, 2009).

Table 5. Estimated diffusion coefficient, Surface Cl- concentration and CTL

Type	Diffusion coefficient	Surface Cl⁻ concentration	Threshold chloride concentration			
	(cm^2/yr)	(kg/m^3)	Min	Avg	Max	% mass of cement content (average)
				(kg/m^3)		
N1P	5.79	21.1	4.7	4.7	4.8	1.9
N2P						
N2PS	2.27	22.6	3.7	5.0	6.6	1.5
N2D	3.10	22.1	1.0	2.3	4.1	0.7

Note: An average of all parameters of N2P and N2PS are presented as the concrete mix proportion is same.

The obtained chloride threshold levels are higher than that could be found in current design codes. Particularly this study aimed to determine chloride threshold level precisely at the stage of initiation focusing on concrete mix proportion and rebars surface finishing. The chloride threshold level also depends on the method used for corrosion initiation detection. Other parameters influencing chloride threshold level (e.g. moisture content, temperature fluctuation, influence of other ions present in sea water, rebars surface finish, laboratory test specimens/real concrete structure) were not taken into consideration. This may be probable cause of higher value obtained for CTL.

3.5. Influence of Ca(OH)2 content on corrosion initiation

Figure 5 shows the DTA graph of one N1 type sample and two N2 type sample and CH content of five concrete samples. An average CH content was found 1.08% and 1.86% for N1 and N2 type concrete respectively.

(a)	(b)
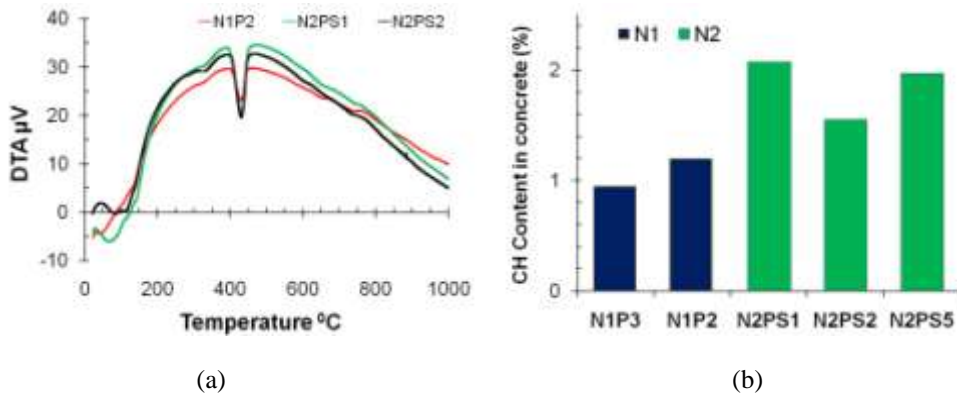
Figure 5 : (a) DTA graph; (b) CH content in different concrete specimens.

It is well known that the CH content in concrete depends on the amount of cement used. A dependency of chloride threshold level with the CH content in concrete was found by expressing them in percentage of concrete. Mass percentage of hydroxide in concrete is found through the gravimetric proportion of Ca^{2+} and OH^- in portlandite. Finally, amount of Cl^- and OH^- present at the vicinity of rebar at the stage of corrosion was correlated. It should be noted that the CTL concentrations are (reported in kg/m^3) converted to percentage of concrete mass considering normal concrete density of 2400 kg/m^3 as the OH^- content obtained are in terms of mass percentage of concrete. An average Cl^-/OH^- ratio of 0.40 and 0.24 was found for N1 and N2 type concrete respectively as criteria for corrosion initiation.

4.0   Conclusion

Reliability of research on Chloride Threshold Level (CTL) determination greatly depends on the accurate detection of corrosion initiation of rebars in concrete. Based on the extensive experimental analysis of this research, the following conclusions were drawn:

a) The lead reference electrode is capable to detect corrosion onset of rebars in concrete accurately through half-cell potential monitoring even at the stage when corrosion current (rate) measured by the portable corrosion meter is as low as 0.002 $\mu A/cm^2$.

b) Chloride threshold level (CTL) of 4.7 and 5.0 kg/m^3 is estimated for N1 and N2 concrete at an average corrosion onset time of 119 and 260 days respectively. Using the same mix proportioned concrete CTL for deformed bar reduced to less than 50% of plain rebar.

c) Corrosion initiation in concrete specimens with lead reference electrode was predicted reliably with a lowest corrosion area of 0.08 cm^2. In the deformed rebars corrosion was spread over a considerable area with a shallow depth even at lower CTL. The rebar corrosion area was found in wider range with various natures of corrosion initiation.

d) Through Thermo-Gravimetry/Differential Thermal Analyzer (TG/DTA) analysis the CH (portlandite) contents were found 1.08 % and 1.86% by mass of concrete in N1 and N2 concrete respectively. A $[Cl^-]/[OH^-]$ ratios of 0.40 and 0.24 for N1 and N2 type concrete respectively were found in mass basis.

Acknowledgement

References

Alonso, C., Castellote, M. and Andrade, C. (2002) Chloride threshold dependence of pitting potential of reinforcements, *Electrochemica Acta*, 47: 3469–3481.

American Society for Testing and Materials (ASTM) (1999) Standard test for half-cell potentials of uncoated reinforcing steel in concrete. ASTM C 876-99, West Conshohocken, USA.

Bertolini, L., Elsener, B., Pedeferri, P. and Polder, R. (2004) Corrosion of steel in concrete: prevention, diagnosis, repair, Weinheim: Wiley-VCH, 409p.

Hansson, C.M. and Sorensen, B. (1990) The threshold concentration of chloride in concrete for initiation of reinforcement corrosion, In Berke N.S., Chaker V. and

Whiting D. (Eds.) *Corrosion Rates of Steel in Concrete, ASTM STP 1065*, 3–16.

Hausmann, D.A. (1967) Steel corrosion in concrete; How does it occur? *Materials and Protection*, 6: 19–23.

Hope, B.B. and Ip, A.K.C. (1989) Corrosion inhibitors for use in concrete, *ACI Material Journal*, 86: 602–608.

Horiguchi, K., Maruya, T. and Takewaka, K. (2006) Estimation of initiation stage for corrosion by half-cell potential and chloride threshold value, *Proceedings of JCI* 28: 1007-1012 (In Japanese).

Horiguchi, K., Maruya, T. and Takewaka, K. (2007) An effect of mix proportion on chloride threshold value, *Proceedings of JCI,* 29: 1377-1382 (In Japanese).

Hussain, S.E., AlGahtani, A.S. and Rasheeduzzafar (1996) Chloride threshold for corrosion of reinforcement in concrete, *ACI Materials Journal*, 93: 534-538.

Japanese Industrial Standards (JIS) (2003) Methods of test for chloride ion content in hardened concrete, JIS A 1154, 472-482, Japan (In Japanese).

Kayyali O.A. and Haque M.N. (1988) Chloride penetration and the ratio of $C\ell^-/OH^-$ in the pores of cement paste, *Cement and Concrete Research*, 18: 895-900.

Mammoliti, L.T., Brown, L.C., Hansson, C.M. and Hope, B.B. (1996) The influence of surface finish of reinforcing steel and ph of the test solution on the chloride threshold concentration for corrosion initiation in synthetic pore solutions, *Cement and Concrete Research*, 26: 545-550.

Manera, M., Vennesland, Ø. and Bertolini, L. (2008) Chloride threshold for rebar corrosion in concrete with addition of silica fume, *Corrosion Science*, 50: 554-560.

Masi, M., Colella, D., Radaelli, G. and Bertolini, L. (1997) Simulation of chloride penetration in cement-based materials, *Cement and Concrete Research*, 27: 1591-1601.

Mohammed, T. U., Otsuki, N. and Hisada, M. (1999) Corrosion of steel bars with respect to orientation in concrete, *ACI Materials Journal*, 96:154-160.

Montemor, M.F., Alves, J.H., Simões, A.M., Fernandes, J.C.S., Lourenço, Z., Costa, A.J.S., Appleton, A.J. and Ferreira, M.G.S. (2006) Multiprobe chloride sensor for in situ monitoring of reinforced concrete structures, *Cement and Concrete Composites*, 28: 233-236.

Page, C.L. (1975) Mechanism of corrosion protection in reinforced concrete marine structure, *Letters to Nature*, 258: 514-515.

Page, C.L. and Treadaway, K.W.J. (1982) Aspects of the electrochemistry of steel in concrete, *Nature*, 297:109-115.

Poursaee, A. and Hansson, C.M. (2009) Potential pitfalls in assessing chloride-induced corrosion of steel in concrete, *Cement and Concrete Research*, 39: 391-400.

Schiessl, P. and Raupach, M. (1990) Influence of concrete composition and microclimate on the critical chloride content in concrete, In Page, C.L., Treadaway, K.W.J. and Bamforth, P.B. (eds.)*, Corrosion of Reinforcement in Concrete,* Elsevier Applied Science, London, 49-58.

Sorn, V., Oshiro, T., Yamada, Y., Sugiyama, T. and Matsufuji, Y. (2001) Performance of fly ash concrete in accelerated and natural chloride exposure regimes, *Proceedings of The Seventh CANMET / ACI International Conference on Fly Ash,*

Silica Fume, Slag, and Natural Pozzolans in Concrete, Malhotra V.M. (eds.), Madras, India, 185-204, .

Thomas, M. (1996) Chloride thresholds in marine concrete, *Cement and Concrete Research*, 26: 513–519.

Tuutti, K. (1982) Corrosion of steel in concrete, Swedish Cement and Concrete Research Institute, Sweden, Stockholm, 486p.

Vassie, P. (1984) Reinforcement corrosion and the durability of concrete bridges, *Proceeding of Institution of Civil Engineers*, 76: 713–723.

Xua, J, Jiang, L. and Wang, J. (2009) Influence of detection methods on chloride threshold value for the corrosion of steel reinforcement, *Construction and Building Materials*, 23: 1902-1908.

Yokota M. (1998) Study on corrosion monitoring of reinforcing steel bars in 36-year old actual concrete structures, *Translation from proceedings of JCI*, 20, (concrete library of JSCE 33, 1999, 155-164).

Yonesawa, T., Ashworth, V. and Procter, R. P. M. (1988) Pore solution composition and chloride effects on the corrosion of steel in concrete, *Corrosion,* 44: 489-499.